Research on Slot-pole Combination in High-power Direct-drive PM Vernier Generator for Fractional Frequency Transmission System

Zhidong Yuan, Shaofeng Jia, *Senior Member, IEEE*, Deliang Liang, *Senior Member, IEEE*, and Xiuli Wang, *Senior Member, IEEE*, and Yong Yang

***Abstract*—Offshore wind energy is an important part of clean energy, and the adoption of wind energy to generate electricity will contribute to the implementation of the carbon peaking and carbon neutrality goals. The combination of the fractional frequency transmission system (FFTS) and the direct-drive wind turbine generator will be beneficial to the development of the offshore wind power industry. The use of fractional frequency in FFTS is beneficial to the transmission of electrical energy, but it will also lead to an increase in the volume and weight of the generator, which is unfavorable for wind power generation. Improving the torque density of the generator can effectively reduce the volume of the generators. The vernier permanent magnet machine (VPM) operates on the magnetic flux modulation principle and has the merits of high torque density. In the field of electric machines, the vernier machine based on the principle of magnetic flux modulation has been proved its feasibility to reduce the volume and weight. However, in the field of low-speed direct-drive machines for high-power fractional frequency power generation, there are still few related researches. Therefore, this paper studies the application of magnetic flux modulation in fractional frequency and high-power direct-drive wind turbine generators, mainly analyzes the influence of different pole ratios and different pole pairs on the generator, and draws some conclusions to provide reference for the design of wind turbine generators.**

***Index Terms*—Direct-drive wind turbine generators, Fractional frequency transmission system, Pole ratio, The magnetic flux modulation, Vernier machine.**

I. INTRODUCTION

WITH the proposal of carbon peaking and carbon neutrality strategy, the proportion of clean energy will be larger and larger in the future. In recent years, wind power has become the fastest growing electric energy source in the world [1]. In general, wind power is divided into onshore and offshore. Due to the limited onshore wind resources and land resources, offshore wind power generation is becoming more and more attractive. One noticeable trend is that the offshore distance of offshore wind turbines is increasing year by year, and the traditional power transmission technique is no longer the best option to meet the needs. The fractional frequency transmission system (FFTS) proposed by Academician Wang Xifan can adapt to long-distance offshore power transmission by lowering the transmission frequency, which is more suitable for offshore wind power generation [2], [3].

In most cases, offshore wind turbines require a multi-stage gearbox to match the speed of the synchronous generator due to the low speed of the turbine [4]. However, gearboxes are often prone to failure and have a limited lifespan, which leads to a reduction in generator reliability[5]. The direct-drive wind turbine is an excellent solution to this problem since its low-speed rotor can be directly coupled to the turbine shaft without the use of a gear transmission system, simplifying the structure and increasing reliability[6]. Therefore, direct-drive wind turbines have become the preferred option for offshore wind power generation [7]. However, the low-speed, high-torque design will inevitably result in a larger volume than regular high-speed machines and brings great challenges to processing, installation, and transportation [8], [9]. Thus, any reduction in generator size (and mass) would be helpful [10]. For FFTS, the operating frequency of the system is decreased even further, which results in a lower generator speed and a further increase in volume. Therefore, improving the power density and further realizing the lightweight of the generator will be the key factors of the FFTS system.

VPM operates with the flux modulation principle, which is similar to a mechanical gear. Therefore, it can obviously increase the torque density and reduce the size of the machine [11]. Therefore, it has a lot of potential in industries that require low-speed, high-torque, and wide-speed operations, like wind power generation, in wheel electric vehicles, and ship drives [12]. Furthermore, it was pointed out that the concentrated winding permanent magnet machine with an open slot also has the magnetic flux modulation effect [13], [14]. For high-power wind turbine generators, an open slot structure is commonly utilized for the convenience of manufacture, so the magnetic flux modulation effect already exists in wind turbine generators

Manuscript received January 31, 2022; revised April 25, 2022; accepted June 02, 2022. date of publication December 25, 2022; date of current version December 18, 2022.

This work was supported by the Science and Technology Foundation of SGCC (5500-202099509A-0-0-00) "Research on Fractional Frequency Transmission Technology for Largely Enhancing Transmission Capacity and Development of Its Key Devices".*(Corresponding Author: Shaofeng Jia)*

Zhidong Yuan, Shaofeng Jia, Deliang Liang, Xiuli Wang are with the State Key Laboratory of Electrical Insulation and Power Equipment, Shaanxi Key Laboratory of Smart Grid, School of Electrical Engineering, Xi'an Jiaotong University, Xi'an, China (e-mail: shaofengjia@ xjtu.edu.cn).

Yong Yang is with State Grid Gansu Electric Power Research Institute, Lanzhou, China.

Digital Object Identifier 10.30941/CESTEMS.2022.00056

in theory. Some researchers have studied the application of VPM in high-power wind turbines with a conventional frequency of 50 Hz [10], [15], but there is a lack of research in the field of high-power fractional-frequency power generation. Therefore, this paper presents a comparative study on the influence of magnetic flux modulation effects on the performance of fractional-frequency high-power direct-drive wind turbine generators.

This paper is organized as follows: the research background and significance of this paper are introduced in Section I. In Section II, the modulation principle of VPM is introduced. Section III analyzes the parameter design principles of the high-power direct-drive generator. Then, in Section IV, the effect of different pole ratios on generator performance is analyzed. Next, Section V selects a generator with a pole ratio of 3.5 and analyzes the effects of different pole pairs. The last part is the conclusion of this paper.

II. Flux Modulation Principle of VPM

Due to the difficulty of maintenance of offshore wind turbine generators, the reliability and availability of generators are primarily considered in the design stage. Therefore, surface-mounted external rotor permanent magnet generators with simple structures and high reliability are commonly used [16], [17]. This Section mainly analyzes the magnetic flux modulation effect in surface-mounted permanent magnet machines.

To facilitate wiring, the stator slots of high-power wind turbine generators are usually set as open slots, as shown in Fig. 1(a). This structure will cause the air-gap permeance to change periodically, which can produce a modulation effect similar to the VPM. The modulation process is shown in Fig. 1(b). Through modulation, the high-order magnetomotive force can form low-order magnetic flux harmonics. Combined with the original high-order magnetic field harmonics, multiple magnetic field harmonics can work at the same time. Taking the 90-slot 140-pole generator as an example, the FFT analysis of the air-gap flux density at no-load is shown in Fig. 2. It can be seen that in addition to the B_{conv} and B_{modu} components, other high-order harmonic components can also contribute to torque creation.

For the surface mounted VPM shown in Fig. 1, the electromagnetic torque can be represented by (1) [18].

$$T_e \approx 3\sqrt{2}k_\omega N_s r_g IL\left(B_{\text{conv}} + \frac{P_r}{P_s}B_{\text{modu}}\right) \tag{1}$$

where k_w is the winding factor, N_s is the number of series turns per phase, I is the effective value of phase current, r_g is the air gap length, L is the machine length, P_s is the pole pairs of armature winding and P_r is the pole pairs of permanent magnet. B_{conv} is the conventional part of the air gap magnetic flux, and its order is equal to the number of pole pairs of the permanent magnet. B_{modu} is generated by the modulation effect, and its order is smaller than the pole pairs of the permanent magnet.

To produce steady electromagnetic torque in a traditional permanent magnet machine, the pole pairs of the stator and rotor must be kept equal, while they are not equal in VPM [19]. The pole ratio (PR) is defined as the ratio of the pole pairs of the rotor to the pole pairs of the stator and can be used to visually express the difference between them [20]. Generally, for the design of VPM, specified number of pole pairs of stator and rotor needs to be satisfied.

$$P_S = \left|Z - P_r\right| \tag{2}$$

where Z is the number of stator slots. Since the number of stator slots and rotor pole pairs of the VPM are relatively close, P_s is usually smaller than P_r. It can be seen from (1) that the torque component generated by B_{modu} is amplified by the pole ratio PR. Therefore, a suitable design can help the machine generate higher torque. It is because of this modulation phenomenon that the VPM becomes a machine with high torque density characteristics.

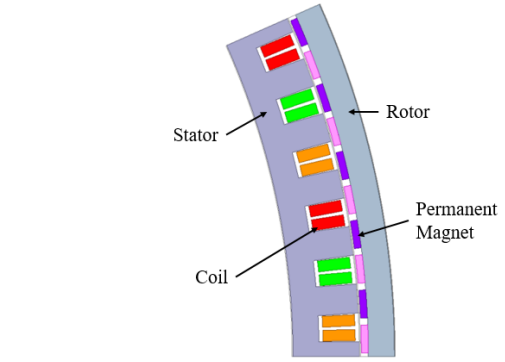

(a)

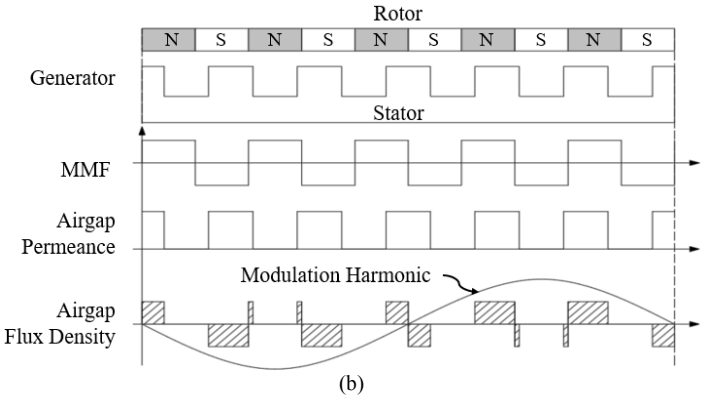

(b)

Fig. 1. Open Slot Surface Mounted Generator model and its flux modulation process. (a) Open slot surface mounted generator model. (b) Flux modulation process of open slot generator.

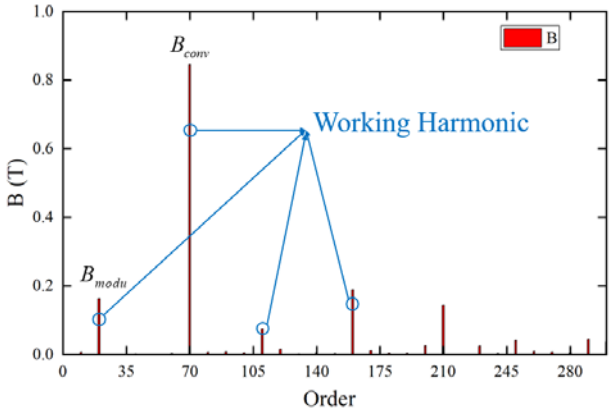

Fig. 2. FFT decomposition of 90-slot 140-pole air-gap flux density.

III. Design Considerations

A. Generator Topology Type

In high-power direct-drive wind turbine generators, the structure of the outer rotor is usually used to generate high torque density. In addition, a simple surface-mounted topology is usually used to facilitate the stability of the structure [21]. The use of stator open slots and parallel teeth design makes it easier to install formed windings [22]. Therefore, the open-slot parallel-tooth external rotor surface-mounted permanent magnet generator is used in this paper.

B. Main Parameters

When comparing different topologies, keep the inner diameter, outer diameter, and air gap length the same, and keep the thermal load, electrical frequency, input power, and materials the same.

The generators designed in this paper all use the electrical frequency of 50/3Hz. The rated speed of the direct-drive wind turbine generator is generally designed between 10-30 rpm. According to formula (3), when the frequency is constant, the rated speed of the generator is inversely proportional to the number of pole pairs. Therefore, the rotation speed needs to be selected according to the combination of slot and pole during design.

$$n = \frac{60f}{P_r} \tag{3}$$

where n is the rotational speed, f is the electrical frequency.

Furthermore, the product of input torque and rotational speed needs to remain the same for all generators, which means that the performance of different schemes is compared at the same input power. The main size of the generator, outer diameter, can be preliminarily calculated from the empirical formula, and then selected according to the size of the existing generator with similar power. The input power of the generator in this paper is about 1.60MW, and the outer diameter of the generator is initially designed to be 4007mm. In large wind turbine generators, the thickness of the magnetic steel is usually designed to be 3 to 7 times the length of the air gap. In this paper, the length of the air gap is 4.5mm, and the thickness of magnetic steel is about 4 times the length of the air gap.

C. Selection of Materials

To improve the generator's reliability, PM materials with good thermal stability and strong anti-demagnetization properties should be chosen. In this paper, 40SH Nd-Fe-B permanent magnet material was selected. The main materials are shown in TABLE I.

TABLE I
Material of the Generator

Components	Winding	Stator Core	Rotor Core	Magnets
Material	Copper	Silicon steel sheet	Silicon steel sheet	Nd-Fe-B
Grade	Rectangular copper wire	50TW400	Low-carbon steel	N40SH_100

IV. Influence of Pole Ratio on Generator Performance

A. Analysis of Different Pole Ratio

Different slot-pole combinations can result in different pole ratios. According to formula (2), the pole ratio is the amplification factor for the torque contributed by the modulating magnetic field. Theoretically, the higher the pole ratio, the higher the torque produced [23]. During the comparison, the number of poles and the rotational speed of the rotor remain the same. By altering the number of stator slots and winding connections, as well as the number of stator magnetic poles, the PR can be varied to study the performance of the system.

B. Design of Machines with Different Pole Ratio

In this comparison, the number of the rotor pole pair is selected to be 70, and the rotational speed is 14.286 rpm. TABLE II lists the slot-pole combinations for comparison. It can be seen that when the number of stator slots decreases, the pole ratio increases. When the pole ratio is greater than 2, the armature winding pitch is greater than 1, indicating that the generator has a distributed winding rather than a centralized winding.

TABLE II
Slot-Pole Combination Corresponding to Different PR

stator slots	Pole pairs of permanent magnets	Armature coil pitch	Winding factor	PR
126	70	1	0.945	1.25
105	70	1	0.866	2
90	70	2	0.945	3.5
84	70	3	1	5

Various performance parameters of the generator can be simulated by finite element analysis (FEA). The FEA models of the generator are shown in Fig. 3, and the main design parameters are shown in TABLE III. It is noteworthy that as the pole ratio increases, the axial length of the generator decreases, and the yoke width of the stator and rotor increases. This indicates that a topology with a big PR requires a broader magnetic path and a shorter axial length for the same input torque.

C. No-load Performance

The cogging torque is shown in Fig. 4. The symbol P1kP2k in the figure refers to the peak-to-peak of the cogging torque. For generators, the small cogging torque makes the starting

TABLE III
Parameter Design Table of Generators With Different PR

Design Parameters	Slot-pole pairs combination			
	126-70	105-70	90-70	84-70
Stator inner diameter (mm)	3600	3600	3600	3600
Stator yoke thickness (mm)	24.3	26.7	44.9	55.3
slot depth (mm)	132.4	132.7	85.6	62.8
Stator tooth width ratio	0.471	0.449	0.374	0.347
Rotor outer diameter	4007	4007	4007	4007
Rotor yoke thickness (mm)	26.3	24	50.5	62.9
PM thickness (mm)	16	15.6	18	18
Polar arc coefficient	0.950	0.893	0.950	0.948
Air gap length (mm)	4.5	4.5	4.5	4.5
Lamination length (mm)	683.0	663.0	600.3	561.0
Conductors per slot	124	78	104	136
Parallel branches	14	7	10	14

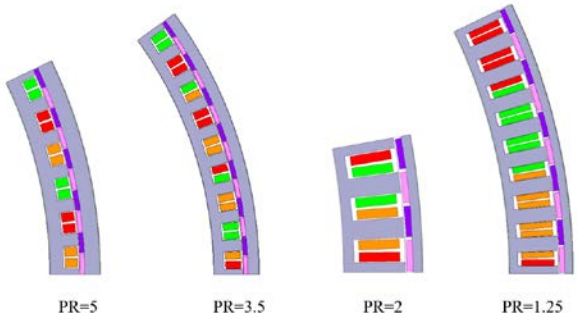

Fig. 3. 2D FEA unit models of generators with different pole ratios (1/14, 1/10, 1/35 and 1/14 model, respectively).

process easier. It can be seen that the cogging torque fluctuation of the 105-slot 140-pole topology and the 126-slot 140-pole topology is large, exceeding 5.6% of the rated torque. When the rotor rotates through a 360° mechanical angle, the fundamental frequency of cogging torque is equal to the least common multiple of the number of stator slots and the number of rotor poles [24]. The number of cogging torques generated in one electrical period is:

$$\lambda = \frac{LCM(z, 2P_r)}{P_r} \tag{4}$$

where λ is the number of cogging torques in one electrical period, $LCM\ (z,\ 2P_r)$ is the least common multiple of the number of slots and the number of magnetic poles. The larger the $LCM\ (z,\ 2P_r)$, the larger the amount of cogging torque fluctuations in one electrical cycle, and the smaller the torque amplitude.[25].

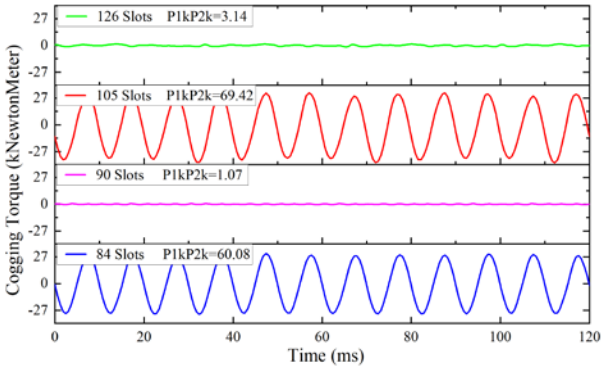

Fig. 4. Comparison chart of cogging torque for machine with different PR.

Fig. 5 shows the air-gap flux density of generators with different PR under no-load conditions. It can be seen that the B_{conv} component decreases with the increase of PR, and the B_{modu} component increases with the increase of PR. This variation trend of the magnetic density value is mainly caused by the different ratios of the tooth widths. When the ratio of the tooth width increases, the modulation effect of the generator weakens, the ratio of the B_{modu} component decreases, and the proportion of B_{conv} increases. In addition, another important difference between the magnetic densities is that a topology with a larger PR has a lower frequency of the B_{modu} component and a higher torque-generating capability, as shown by equation (1).

D. Load Performance

The torque under load is shown in Fig. 6. It can be seen that

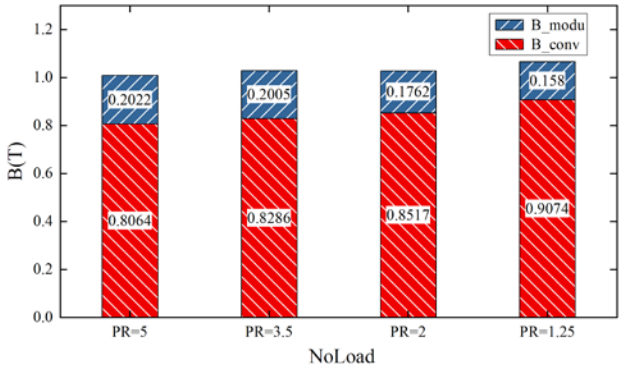

Fig. 5. Air-gap flux density of generators with different PR under no-load conditions.

all the topologies reach the rated torque. The torque fluctuation of the 84-slot 140-pole and 105-slot 140-pole topologies is relatively large, which is consistent with their cogging torque amplitude phenomenon. The load flux density distribution is shown in

Fig. 7. It can be seen that the flux density distribution of these topologies is good.

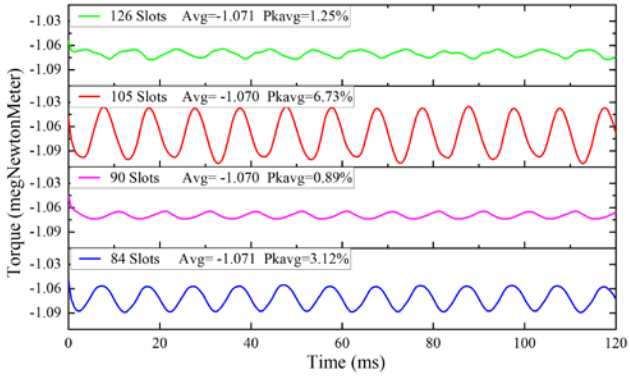

Fig. 6. Load torque for generators with different PR.

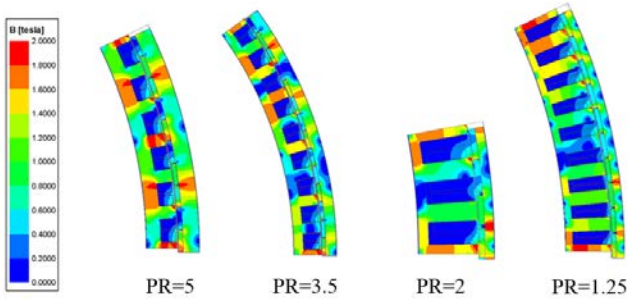

Fig. 7. Flux density distribution of generators with different PR under load.

Fig. 8 shows the air-gap flux density of generators with different PR under load conditions. The air-gap flux density under load is jointly generated by the magnetic steel and the armature winding. In Fig. 8, B_f1 and B_f2 are the flux density components equal to the B_{conv} and B_{modu} orders, respectively. It can be seen that from no-load to load, the B_{conv} component increases slightly for all generators, while the B_{modu} component increases significantly for generators with larger PR. This is because the B_{modu} component order of the generator with large PR is lower, and the amplitude of the low-order flux density generated by the armature winding under the same thermal load is larger. Large-amplitude magnetic flux density is advantageous for generating large torque, but it requires a wider magnetic path.

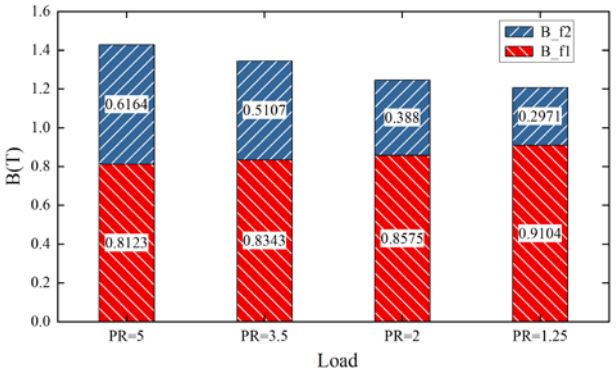

Fig. 8. Air-gap flux density of generators with different PR under load conditions.

TABLE IV shows some electromagnetic properties of the generator under rated conditions.

TABLE IV
ELECTROMAGNETIC PERFORMANCE COMPARISON OF GENERATORS WITH DIFFERENT PR

Electromagnetic properties	Number of slots			
	126	105	90	84
PR	1.25	2	3.5	5
Armature current (A)	1164.5	1150.3	1216.8	1217.5
No-load voltage(V)	477.4	477.1	451.9	460.7
Single phase resistance (ohm)	0.0143	0.0146	0.0157	0.0206
Copper loss (kW)	58.02	58.00	69.84	89.65
Iron loss (kW)	6.53	6.16	5.05	5.55
PM Eddy loss (kW)	3.45	5.89	14.52	14.84
Output Power (MW)	1.532	1.530	1.511	1.490
Efficiency (%)	95.75	95.63	94.44	93.12
Power factor	0.610	0.559	0.453	0.360

By adjusting the number of winding turns, armature current, and number of parallel branches, the no-load voltage of the generator can be adjusted. It can be seen that the no-load voltage of these generators is close.

It can be seen from the loss data that in the fractional frequency direct-drive wind turbine generator, the iron loss accounts for a small proportion, and the main losses are copper losses. The iron loss is positively correlated with the frequency of the magnetic flux. When the fractional frequency is used, the iron loss of the generator is reduced. The large PM eddy current loss is mainly due to the modulation effect of the generator. Besides, it can be seen that the PM eddy current loss increases with the increase of PR, that is, with the increase of the modulation effect. This is because the larger the PR, the stronger the modulation effect and the larger the change in the magnetic flux density in the permanent magnet. Besides, it can be seen from the copper loss data that when the PR is greater than 2, the copper loss will increase significantly, which corresponds to the change in single-phase resistance.

For the efficiency, it can be seen that under the same input power, the output power and efficiency of the generator decrease with the increase of PR. This is mainly related to the change in the loss of the generator. The power factor of the generator drops as PR increases and the power factor reduces dramatically when the pole ratio exceeds 2.

E. Material Consumption and Total Weight

The comparison table of the material weight of each part is shown in TABLE V. It can be seen that the total weights of all topologies are almost equal, but the topology with a large PR has a small weight of the stator iron core and a large weight of the rotor iron core. This is because a topology with a large PR has a short axial length, but a wider magnetic path and longer winding end. Under the comprehensive influence, the total weight shows an equal trend.

TABLE V
MATERIAL WEIGHT COMPARISON TABLE OF DIFFERENT PR TOPOLOGIES

Slots	PR	Magnet (p.u.)	Stator Core (p.u.)	Rotor Core (p.u.)	Windin g (p.u.)	Total (p.u.)
84	5	0.927	0.930	1.160	0.977	1.003
90	3.5	1	1	1	1	1
105	2	0.911	1.240	0.528	1.160	0.998
126	1.25	1.024	1.314	0.598	1.082	1.037

(Note: The data in the table takes the 90-slot 140-pole machine as the reference group, its material consumption is all set to the reference value 1, and the values of other generators are the relative values of the reference group.)

F. Selection of Optimal PR Based on Dispersion Method

The dispersion method is a typical data normalization approach in which the original data is transformed linearly. This method can be used to assess multi-index systems. The data conversion formula for this method is

$$X = \frac{x_1 - x_{\min}}{x_{\max} - x_{\min}} \tag{5}$$

where x_1 is the current data, x_{min} and x_{max} are the minimum and maximum data in all data, X is the conversion result.

Since the weights of the generators with different PR in this paper are almost the same, and the inner and outer diameters of them are also the same, two main metrics are considered: axial length and power factor, where the axial length can characterize the volume of the generator. Furthermore, the smaller the axial length and the higher the power factor, the better for the generator, so the standardized result of the axial length needs to be adjusted using formula (6).

$$X = (1 - X) \tag{6}$$

The conversion table of the two indicators is shown in TABLE VI, where X and Y represent the axial length and power factor of different schemes. Xscore and Yscore represent normalized results. Finally, when the weight of both indicators is set to 0.5, the total Score can be obtained by formula (7).

$$TotalScore = 0.5 \cdot Xscore + 0.5 \cdot Yscore \tag{7}$$

TABLE VI
VOLUME AND POWER FACTOR CONVERSION TABLE

Scheme Name	S1	S2	S3	S4
PR	1.25	2	3.5	5
X (Axial Length)	683	663	600.3	561
Y (Power Factor)	0.61	0.559	0.453	0.36
Xscore	0	0.164	0.678	1
Yscore	1	0.796	0.372	0
Total Score	0.500	0.480	0.525	0.500

It can be seen that the total score of PR = 3.5 is the largest. In addition to the volume and power factor, the generator with PR=3.5 has the smallest cogging torque and the smallest rated torque ripple, and the efficiency is also at a good level, so this

scheme is finally recommended.

V. Selection of Pole Pairs of Permanent Magnets

A. Analysis of Different Pole Pairs of PM

The pole number selection strategies for conventional induction machines and permanent magnet machines have been introduced in many literatures [26]. In high-power permanent magnet direct-drive wind turbines, the operating speed of the generator is as low as 10-30rpm, and the generator's number of pole pairs can range from tens to hundreds. In general, when the number of magnetic poles increases, the thickness of the generator yoke can be reduced, and it will have a higher power density. However, with the increase of magnetic poles, the magnetic leakage will become stronger, and the reducing effect on the yoke will become smaller. This shows that there is an optimal value for the number of magnetic poles and it is significant to optimize the number of poles, which can be selected in a wide range.

B. Design of Machines with Different Pole Pairs of PM

When comparing the performance of generators with different pole pairs, it is necessary to keep the main variables of the generator the same, such as input power, PR, thermal load, and inner and outer diameter, and observe how the generator's performance changes under different pole pairs, such as volume, power factor, flux density distribution, etc. In this paper, a generator with a pole ratio of 3.5 is selected for comparison. A total of four generators are designed, and their slot pole combinations are shown in TABLE VII. Since the output electrical frequency remains unchanged, the generator speed will change correspondingly when the number of pole pairs changes. In order to keep the input power consistent, the product of the input torque and the speed should be kept the same. In addition, these generators use the same materials, and all design parameters meet the design requirements. Fig. 9 shows the simulation model of a 72-slot 112-pole generator. Other schemes' models are similar, but only the size has changed, so this Section didn't list them all.

TABLE VII
Slot-pole Combination Scheme with Different Magnetic Pole Pairs

Slot-pole combination	PR	Rotating speed(rpm)	Expected torque (MNm)
108-168	3.5	11.905	1.28
90-140	3.5	14.286	1.07
72-112	3.5	17.857	0.856
54-84	3.5	23.810	0.642

The design parameters of different schemes are shown in TABLE VIII. It can be seen that when the number of pole pairs decreases, the thickness of the stator and rotor yokes gradually increases, and the axial length shows a decreasing trend. This is because when the number of pole pairs of the PM decreases, the number of stator magnetic poles also decreases, the mechanical angle of each armature magnetic pole increases, and the magnetic flux path becomes longer, increasing the flux density of the tooth and yoke, so the magnetic path needs to be widened. The reason for the change in axial length will be analyzed in part D.

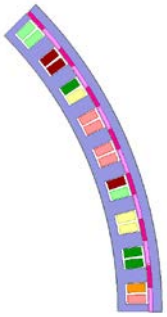

Fig. 9. FEA model of 72-slot 112-pole generator (1/8 model).

TABLE VIII
Parameter Design of Different Magnetic Pole Pairs

Design Parameters	Slot-pole combination			
	108-168	90-140	72-112	54-84
Stator inner diameter (mm)	3600	3600	3600	3600
Stator yoke thickness (mm)	37.4	44.9	54.2	70.0
Slot depth (mm)	102.4	85.6	65.4	35.5
Stator tooth width ratio	0.387	0.374	0.357	0.301
Rotor outer diameter (mm)	4007	4007	4007	4007
Rotor yoke thickness (mm)	41.2	50.5	61.4	75.5
PM thickness (mm)	18	18	18	18
Polar arc coefficient	0.95	0.95	0.95	0.919
Air gap length (mm)	4.5	4.5	4.5	4.5
Lamination length (mm)	708	600.3	519	536.8
Conductors per slot	110	104	90	224
Parallel branches	12	10	8	6

C. No-load Performance

The cogging torque of each topology is shown in Fig. 10. It can be seen that the fluctuation amplitude of the cogging torque is very small, less than 0.42% of the rated torque, especially for the 90-slot scheme, where the cogging torque fluctuation is under 0.1 percent of the rated torque. This phenomenon also satisfies the principle of cogging torque mentioned in the previous Section.

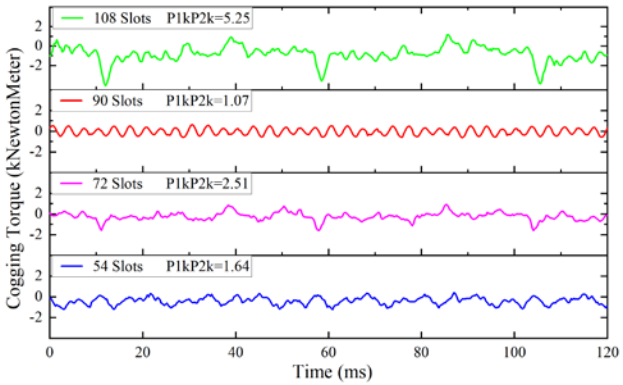

Fig. 10. Cogging torque for different pole pairs topologies.

Fig. 11 shows the air-gap flux density of generators with different pole pairs at no-load. It can be seen that the ratios of B_{conv} to B_{modu} of these generators are different, which is also

caused by the different ratios of the tooth widths. In addition, the frequencies of the B_{modu} components of these schemes are also different. When the PR is the same, the fewer the number of poles, the lower the frequency of the B_{modu} components.

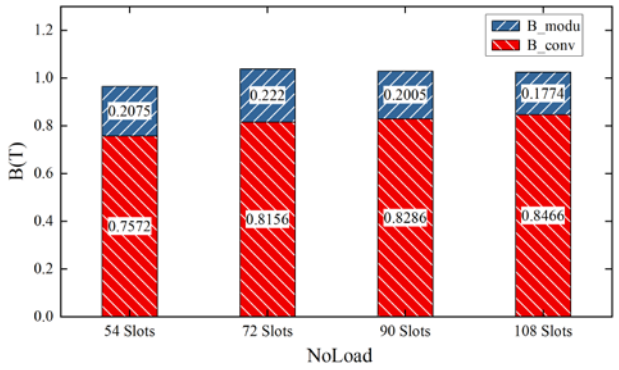

Fig. 11. Air-gap flux density under no-load condition with PR=3.5.

D. Load Performance

The torque under load conditions is shown in Fig. 12. It can be seen that the torque of all generators reaches the expected torque, and the torque ripple is at a good level. The flux density distribution of the load is shown in Fig. 13, and it can be seen that the flux density distribution of all generators is good.

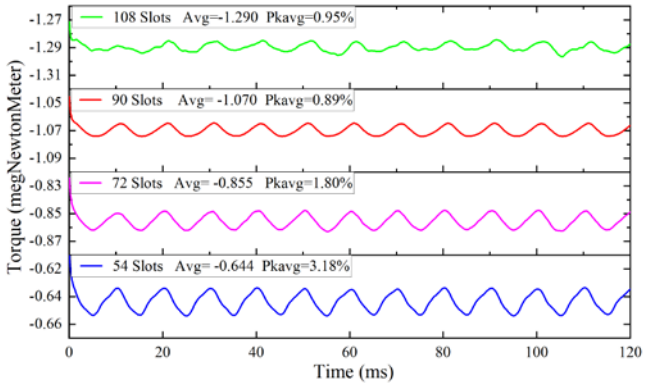

Fig. 12. Load torque for different pole pairs topologies.

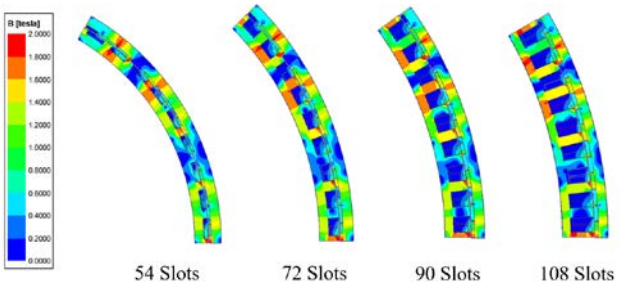

Fig. 13. Load flux density distribution of different pole pairs topologies.

Fig. 14 shows the air-gap flux density ratio of generators with different pole pairs under rated load. It can be seen that the low-order harmonic components B_f2 of these generators all increase significantly compared to the no-load condition, and the increase value is almost the same. Although the reduction of the number of poles is conducive to the generation of a large magnetic density, the speed of the rotor increases with the reduction of the number of pole pairs. Therefore, the speed of the low-order harmonic B_f2 is almost the same, and the amplitude of the low-order harmonic generated by the armature winding is almost the same. The difference in their values is mainly due to the difference in the stator tooth width ratio and the pole arc coefficient of the PM, which means that their ability to generate torque is different. In addition, since the expected torque of generators with a lower number of pole pairs is smaller, their axial length shows a decreasing trend.

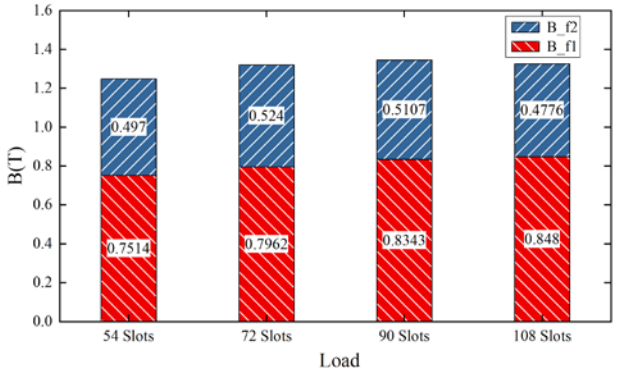

Fig. 14. Air-gap flux density under load condition with PR=3.5.

The electromagnetic performance of generators with different pole pairs is summarized in Table X. The phenomenon of armature current and the induced voltage is the same as the analysis in the previous part. It can be seen from the loss data that the PM eddy current loss increases as the number of pole pairs decrease. This is because when the number of pole pairs decreases, the circumferential area of a single magnet increases, and it is easier to induce large eddy currents. Furthermore, it can be seen that under the same input power, the output power and efficiency of the generator decrease as the number of pole pairs decreases, which is mainly due to the eddy current loss of the permanent magnet. In addition, the power factor increases as the number of pole pairs decrease.

TABLE IX
ELECTROMAGNETIC PERFORMANCE OF GENERATORS WITH DIFFERENT POLES

Electromagnetic properties	Slot-pole combination			
	108-168	90-140	72-112	54-84
Armature current (A)	1242.3	1216.8	1241.7	1242.3
No-load voltage(V)	472.9	451.9	452.5	449.2
Single phase resistance (ohm)	0.0158	0.0157	0.0151	0.0212
Copper loss (kW)	73.2	69.84	69.7	81.8
Iron loss (kW)	5.94	5.05	4.29	4.11
PM Eddy loss (kW)	11.30	14.52	32.66	57.32
Output Power (MW)	1.510	1.511	1.493	1.457
Efficiency (%)	94.37	94.44	93.31	91.06
Power Factor	0.428	0.453	0.487	0.494

E. Comparison of Torque Density

The torque densities of the four generators, as well as the weight of each component, are compared in TABLE X. It can be seen that the total weight of the generator tends to decrease as the number of pole pairs decreases. This is because the axial length of the generator tends to decrease as the number of pole pairs decreases, but the yoke width needs to be widened. Under the combined effect, the total weight of the generator shows a decreasing trend as the number of pole pairs decreases.

Furthermore, the torque density of the generator increases as

the number of pole pairs increases, as shown in TABLE X. However, when the number of slots is greater than 108, the wind turbine's rotational speed drops a lot, and the generator's size and weight increase. Considering that the rated speed of the generator should not be too low, and considering parameters such as torque density, cogging torque, power factor, torque fluctuation, etc., the 90-slot 140-pole scheme is recommended finally in this paper.

TABLE X
TORQUE DENSITY COMPARISON TABLE OF DIFFERENT NUMBERS OF POLES

Slots	Magnet Weight (p.u.)	Stator Core (p.u.)	Rotor Core (p.u.)	Winding Weight (p.u.)	Total Weight (p.u.)	Torque Density (p.u.)
54	0.854	0.926	1.328	0.543	0.933	0.645
72	0.860	0.866	1.048	0.779	0.893	0.894
90	1	1	1	1	1	1
108	1.185	1.190	1.328	1.222	1.137	1.060

(Note: The data in the table takes the 90-slot machine as the reference group, its material consumption is all set to the reference value 1, and the values of other generators are the relative values of the reference group.)

VI. CONCLUSION

The impact of various slot-pole combinations on the operation of fractional-frequency high-power wind turbines is studied in this paper from the perspective of magnetic flux modulation effect. Firstly, the parameter design concerns for a high-power direct-drive wind turbine is analyzed. Then, an experiment was designed to compare the effects of different pole ratio. Next, a generator with a pole ratio of 3.5 was selected to compare the effects of different pole pairs.

The study found that the axial length of a generator with a big pole ratio is shorter, but the yoke width is wider. The iron loss accounts for a minor amount of the total loss in fractional-frequency direct-drive VPM; the main loss is copper loss, and the PM eddy current loss grows as the pole ratio increases. Furthermore, the overall weight of generators with different pole ratios is about the same, and the generator's power factor drops as the pole ratio increases. Using the dispersion method to calculate the two primary indicators of power factor and volume, and considering parameters such as cogging torque, rated torque ripple, and efficiency, it is determined that PR = 3.5 is a good scheme. Finally, considering the turbine speed, machine torque density, weight, and efficiency, the scheme of 90 slots and 140 poles VPM is recommended in this paper, which is more suitable for offshore frequency division transmission system.

REFERENCES

[1] F. Blaabjerg and K. Ma. "Wind Energy Systems," in *Proceedings of the IEEE*, vol. 105, no. 11, pp. 2116-2131, Nov. 2017.

[2] X. Wang, X. Wei, L. Ning and X. Wang, "Integration Techniques and Transmission Schemes for Off-shore Wind Farms," *Proceedings of the CSEE,* vol.34, no.31, pp.5459-5466, Nov.5, 2014.

[3] S. Liu, X. Wang, L. Ning, B. Wang, M. Lu and C. Shao, "Integrating Offshore Wind Power Via Fractional Frequency Transmission System," *IEEE Transactions on Power Delivery*, vol. 32, no. 3, pp. 1253-1261, June 2017.

[4] E. Taherian-Fard, R. Sahebi, T. Niknam, A. Izadian and M. Shasadeghi, "Wind Turbine Drivetrain Technologies," in *IEEE Transactions on Industry Applications*, vol. 56, no. 2, pp. 1729-1741, March-April 2020.

[5] Z. Hu, Y. Wu, R. Li, H. Xin, Y. Yang and J. Wang, "Fault diagnosis of wind turbine gearbox at different operating zones," *2019 IEEE Sustainable Power and Energy Conference (iSPEC)*, Beijing, China, 2019, pp. 578-583.

[6] R.S. Semken, M. Polikarpova, P. Roytta, et al, "Direct-drive permanent magnet generators for high-power wind turbines: benefits and limiting factors", *IET Renewable Power Generation*, 6 (1), 1–8 (2012).

[7] X. Yin, Y. Fang, X. Huang, and P. Pfister, "Analytical Modeling of a Novel Vernier Pseudo-Direct-Drive Permanent-Magnet Machine," *IEEE Transactions on Magnetics*, vol. 53, no. 6, pp. 1-4, June 2017, Art no. 7207404.

[8] Z. Zhang, A. Chen, A. Matveev, R. Nilssen, and A. Nysveen, ''High-power generators for offshore wind turbines,'' *Energy Procedia*, vol. 35, pp. 52–61, Jan. 2013.

[9] J. Shen, X. Qin and Y. Wang, "High-speed permanent magnet electrical machines — applications, key issues and challenges," *CES Transactions on Electrical Machines and Systems*, vol. 2, no. 1, pp. 23-33, March 2018.

[10] D. K. K. Padinharu, G. -J. Li, Z. -Q. Zhu, R. Clark, A. S. Thomas and Z. Azar, "System-Level Investigation of Multi-MW Direct-Drive Wind Power PM Vernier Generators," *IEEE Access*, vol. 8, pp. 191433-191446, 2020.

[11] Y. Liu and Z. Q. Zhu, "Magnetic gearing effect in vernier permanent magnet synchronous machines," *2017 IEEE Energy Conversion Congress and Exposition (ECCE)*, Cincinnati, OH, USA, 2017, pp. 5025-5032.

[12] H. Lin, Y. Zhang, H. Yang, S. Fang and Y. Huang. "Overview and Recent Developments of Permanent Magnet Vernier Machines," *Proceedings of the CSEE,* vol.36, no.18, pp.5021-5034, Sep. 20, 2016.

[13] D. Li, T. Zou, R. Qu and D. Jiang. "Analysis of Fractional-Slot Concentrated Winding PM Vernier Machines with Regular Open-Slot Stators." *IEEE Transactions on Industry Applications*, vol.54, no.2, pp.1320-1330, March-April 2018.

[14] Y. Ma and W. N. Fu, "Design and Comparison of Vernier Permanent-Magnet Machines With Different Winding Types Based on Fractional-Slot Windings," *IEEE Transactions on Magnetics*, vol. 57, no. 6, pp. 1-5, June 2021

[15] D. K. K. Padinharu et al., "Permanent Magnet Vernier Machines for Direct-Drive Offshore Wind Power: Benefits and Challenges," *IEEE Access*, vol. 10, pp. 20652-20668, 2022.

[16] I. Boldea, "Electric generators and motors: An overview," *CES Transactions on Electrical Machines and Systems*, vol. 1, no. 1, pp. 3-14, March 2017.

[17] V. Yaramasu, B. Wu, P. C. Sen, S. Kouro and M. Narimani, "High-power wind energy conversion systems: State-of-the-art and emerging technologies," in *Proceedings of the IEEE*, vol. 103, no. 5, pp. 740-788, May 2015.

[18] T. Zou, D. Li, R. Qu and D. Jiang, "Performance Comparison of Surface and Spoke-Type Flux-Modulation Machines With Different Pole Ratios," *IEEE Transactions on Magnetics*, vol. 53, no. 6, pp. 1-5, June 2017

[19] B. Kim, "Design Method of a Direct-Drive Permanent Magnet Vernier Generator for a Wind Turbine System," in *IEEE Transactions on Industry Applications*, vol. 55, no. 5, pp. 4665-4675, Sept.-Oct. 2019.

[20] B. Kim, "Design of a Direct Drive Permanent Magnet Vernier Generator for a Wind Turbine System," *2018 IEEE Energy Conversion Congress and Exposition (ECCE)*, Portland, OR, USA, 2018, pp. 4275-4282.

[21] T. Z. Htet, Z. Zhao and Q. Gu, "Design analysis of direct-driven PMSG in wind turbine application," *2016 International Conference on System Reliability and Science (ICSRS)*, Paris, France, 2016, pp. 7-11.

[22] C. He and T. Wu, "Analysis and design of surface permanent magnet synchronous motor and generator," *CES Transactions on Electrical Machines and Systems*, vol. 3, no. 1, pp. 94-100, March 2019.

[23] J. T. Shi and Z. Q. Zhu, "Influence of inner/outer stator pole ratio and relative position on electromagnetic performance of partitioned stator switched flux permanent magnet machines," *CES Transactions on Electrical Machines and Systems*, vol. 3, no. 3, pp. 259-268, Sept. 2019.

[24] W. Zhang, J. Gao, L. Dai and S. Huang, "Analysis of magnetic field and torque for all-harmonic-torque motor with surface-mounted permanent magnets," *CES Transactions on Electrical Machines and Systems*, vol. 2, no. 1, pp. 175-180, March 2018.

[25] X. Wang, "Permanent magnet motor," in *China Electric Power Press*, 2nd ed. China: Beijing, 2011.

[26] H. -J. Shin, J. -Y. Choi, Y. -S. Park, M. -M. Koo, S. -M. Jang and H. Han, "Electromagnetic Vibration Analysis and Measurements of Double-Sided Axial-Flux Permanent Magnet Generator with Slotless Stator," *IEEE Transactions on Magnetics*, vol. 50, no. 11, pp. 1-4, Nov. 2014.

Zhidong Yuan was born in Sichuan, China. He received the B.Eng. degree from Zhengzhou University, China, in 2021. He is currently pursuing the M.S. degree in electrical engineering in Xi'an Jiaotong University, Xi'an, China. His research interests include design and optimization of novel permanent magnet and reluctance machines.

Shaofeng Jia (S'14–M'17-SM'21) was born in Shaanxi, China. He received the B.Eng. degree from Xi'an Jiaotong University, Xi'an, China, in 2012, and the Ph.D. degree from the Huazhong University of Science and Technology, Wuhan, China, in 2017, both in electrical engineering. He is currently an Associate Professor with the School of Electrical Engineering, Xi'an Jiaotong University. He is the Author/Co-author of about 70 IEEE technical papers. His research interests include design and control of novel permanent magnet and reluctance machines.

Deliang Liang (M'11–SM'14) received the B.S., M.S., and Ph.D. degrees in electrical engineering from Xi'an Jiaotong University, Xi'an, China, in 1989, 1992, and 1996, respectively. From 2001 to 2002, he was a Visiting Scholar in the Science Solution International Laboratory, Tokyo, Japan. Since 1999, he has been in the Department of Electrical Engineering, Xi'an Jiaotong University, where he is currently a Professor. His current research interests include optimal design, control, and simulation of electrical machines, and electrical machine technology in renewable energy.

Xiuli Wang (SM) received the B.S., M.S., and Ph.D. degrees in electrical engineering from Xi'an Jiaotong University, Xi'an, China, in 1982, 1985, and 1997, respectively, where she is currently a Professor with the School of Electrical Engineering. Her current research interests include power market, reliability assessment of power system, and integration of renewable power.

Yong Yang was born in Gansu, China. He received the B.Eng. degree from North China Electric Power University, China, in 1995. Currently, he is the director of State Grid Gansu Electric Power Company Electric Power Research Institute, Lanzhou, China. His current research interests include power system analysis, relay protection, and renewable energy grid-connected technology.